

1 **Estimating the Location of Scatterers Using Correlation of Scattered Rayleigh Waves**

2 U. Harmankaya^{1*}, A. Kaslilar¹, K. van Wijk², K. Wapenaar³, D. Draganov³

3 ¹ Department of Geophysical Engineering, Faculty of Mines, Istanbul Technical University, 34469,
4 Istanbul, Turkey

5 ² Department of Physics, University of Auckland, New Zealand

6 ³ Sec. Applied Geophysics and Petrophysics, Dept. of Geoscience & Engineering, Delft University of
7 Technology, The Netherlands

8

9

10 **Main objectives:**

11 We use a technique inspired by seismic interferometry and estimate the locations of near-surface scatterers
12 by correlation and inversion of scattered Rayleigh waves.

13 **New aspects covered :**

14 We illustrate the potential of the method when many scatterers are present in the medium. We estimate the
15 location of the scatterers with ultrasonic laboratory measurements of scattered Rayleigh waves

16

17 **SUMMARY**

18

19 Inspired by a technique called seismic interferometry, we estimate the location of scatterers in a scaled
20 model, where many near-surface scatterers are present. We isolate the scattered wavefield and evaluate
21 correlation of scattered waves at different receiver locations. The cross-correlation eliminates the travel
22 path between a source and a scatterer, making the estimation of the scatterers' locations dependent only on
23 properties between the receivers and the scatterer. We illustrate the potential of this method by locating
24 scatterers with ultrasonic laboratory measurements of scattered Rayleigh waves recorded on two parallel
25 and orthogonal lines of receivers. As near-surface scatterers are potential weak zones and may pose risk
26 for the environment, to mitigate geo and environmental hazards, this method can be an efficient alternative
27 that can be used in detection of such structures.

28

Introduction

The Earth's subsurface contains heterogeneities at different scales. When seismic waves encounter inhomogeneities they may scatter. Scattered surface waves can be used for locating and characterizing near-surface structures at engineering scale (e.g., *Grandjean and Leparoux, 2004; Xia et al., 2007; Harmankaya et al., 2013*) and at exploration and global scale (e.g., *Sniieder and Nolet, 1987; Rickers et al., 2012*). Here, we utilize only scattered surface waves at the receivers due to one source at the surface and perform correlation. Interpreting this process from the point of view of seismic interferometry, when one source is present and only scattered fields are correlated, only non-physical (ghost) arrivals will be retrieved (*Harmankaya et al., 2013, Mikesell et al., 2009; Meles and Curtis, 2013*). Here, we use such correlations of scattered arrivals to estimate the location of scatterers. We apply the method to ultrasonic laboratory data collected on an aluminum block, which data is representative for geophysical field studies, and estimate the location of scatterers with good accuracy.

Estimation of the Location of Scatterers

We apply the method given in *Harmankaya et al. (2013)* to a part of an ultrasonic dataset. In Figure 1, the laser ultrasonic-data acquisition geometry is given. The triangles represent the receiver lines with sampling of 1 mm, and S (the star) represents the source. The data are collected on an aluminum block with the irregularly located scatterers being cylindrical holes with a diameter of 1 mm and depth of 30 mm. The Rayleigh velocity in aluminum is 2900 ms^{-1} .

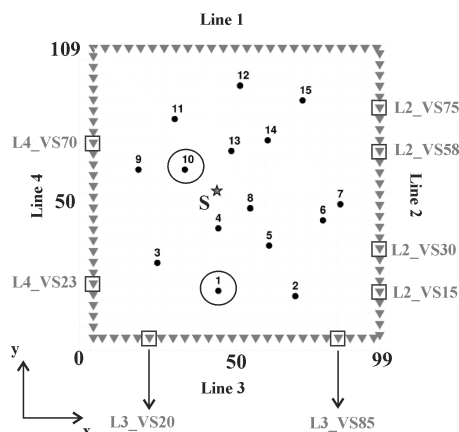


Figure 1. Top view of the ultrasonic laboratory set up: the source (star), receivers (triangles) and scatterers (dots). The triangles in box are the virtual-source locations with the related short-hand notations (see text). The scatterers, whose locations are estimated, are given in circles (1 and 10). The left bottom corner is set as the origin of the acquisition geometry.

This dataset is also used by *Mikesell et al., (2012)* to estimate the location (x and y coordinates) of the scatterers. As the authors aimed to retrieve physical arrivals from seismic interferometry, they autocorrelated the complete wavefield (direct and scattered) recordings at the receivers from the source at S and summed over the enclosing receivers (four lines). When the aim is not to retrieve complete Green's function, but just locate the scatterers, our method could be seen as an effective alternative. It can work with irregular distribution of receivers provided that the scattered wavefield is isolated from the total wavefield.

In our method, we take the recordings at the receivers from the source and isolate the scattered wavefield only. We select a reference trace at the virtual-source (VS) location and correlate all the traces on the isolated scattered wavefield with the trace at the VS location. This eliminates the common travel path from the source to the scatterer and results in the retrieval of a ghost (non-physical) scattered body or surface waves. The location of the scatterer (x and y), is estimated by inverting for the following ghost travel-time relation:

$$t = \frac{1}{V} \left\{ \left[(x_i^r - x)^2 + (y_i^r - y)^2 \right]^{1/2} - \left[(x^{VS} - x)^2 + (y^{VS} - y)^2 \right]^{1/2} \right\}, \quad (1)$$

where r denotes the receiver and i is the receiver index.

Here, we consider an open receiver boundary and use the parallel receiver lines 2 and 4 in Figure 1. As the scatterers are off the lines of receivers, to estimate the location of the scatterers two receiver lines are required. The receivers in the boxes represent the VS locations with shorthand notations such that L2_VS75 indicates line 2 (L2) and the VS at receiver 75. To estimate the x- and y-coordinate of the scatterer with scattered Rayleigh waves (Figures 2a and 3a), we select at both receiver lines the scattered arrivals that correspond to a scatterer and mute the other arrivals (Figures 2b and 3b). We then choose VS locations to obtain ghost scattered arrivals needed for the inversion. For selected VS locations (VS75 and VS30 for L2 and VS70 and VS23 for L4), the trace at that receiver is cross-correlated with the traces on the muted scattered wavefield (Figures 2b and 3b). In this way, the ghost scattered surface waves are retrieved (Figure 2 and 3c-d). To perform the inversion, the travel times of the retrieved ghost arrivals are picked (dots in Figure 4a and 4b). The inverse problem is solved using damped singular value decomposition. For the two receiver lines, the matrix-vector form is prepared as $[\Delta d_1 \ \Delta d_2]^T = [G_1 \ G_2]^T \Delta \mathbf{m}$, where 1 and 2 correspond to each receiver line and T represents transpose. The vector $\Delta \mathbf{d} = \mathbf{t}^{obs} - \mathbf{t}^{calc}$ is the difference between an observed ghost arrival time, t^{obs} , and a calculated one, t^{calc} , on the basis of an assumed scatterer position (equation 1). The unknown coordinates (x and y) of the scatterer are denoted by the vector $\Delta \mathbf{m}$, while the Jacobian (sensitivity) matrix is represented by \mathbf{G} . To calculate the uncertainties of the estimations, the model covariance matrix is used by considering a coverage factor 2, which provides a confidence level of 95%.

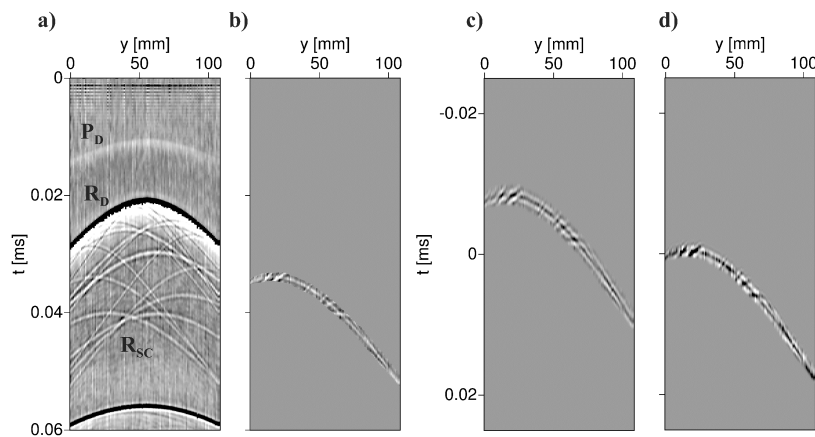


Figure 2. (a) Recorded wavefields along Line 2 due to the source at S. The direct compressional (P_D) and Rayleigh (R_D) waves and the scattered wavefields due to the scatterers (R_{SC}) are clearly observed. (b) Selected scattered Rayleigh-wave arrival due to a scatterer (scatterer 1 in Figure 1). Ghost arrivals retrieved by seismic interferometry applied to (b) for the virtual sources at (c) VS75 and (d) VS30.

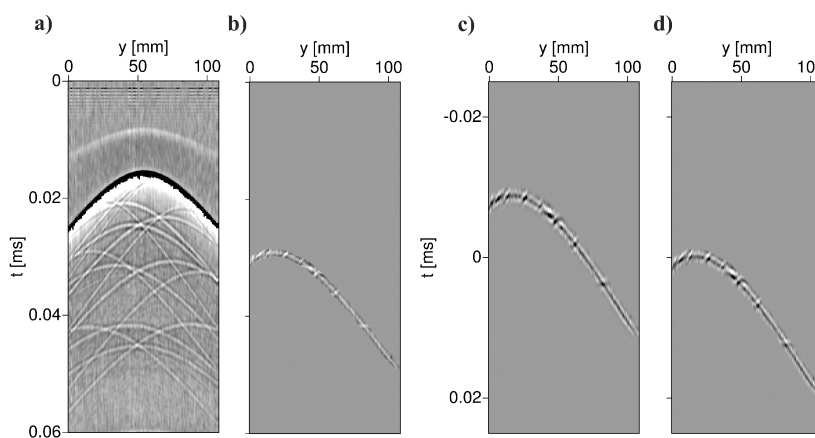


Figure 3. (a) and (b) As in Figure 2, but along line 4. (c) and (d) As in Figure 2, but for VS70 and VS23, respectively.

The travel-time inversion is performed for the couples L2_VS75-L4_VS70 and L2_VS30-L4_VS23 and the location of the scatterer 1 (Figure 1) is estimated (Table 1). The third row in Table 1 gives the average value of the couples. The updates of the model parameters after each iteration are given in Figure 4c. The picked (observed) ghost travel times are plotted together with the calculated ones in Figure 4a for L2_VS75-30 and in Figure 4b for L4_VS70-23. Good agreement between the observed and the calculated travel times (Figure 4a and b) and the actual and the estimated locations (Table 1) are obtained. The agreements are quantified by calculating the normalized percentage errors for the travel time and the estimated model parameters and are given in Table 1.

For the second example, we choose two orthogonal lines, L2 and L3, and apply the same procedures and we estimate the location of scatterer 10 (Figure 1). The travel-time inversion is performed for the couples L2_VS15-L3_VS85 and L2_VS58-L3_VS20; the results are listed in Table 1. From the results in the table, we can conclude that for both the parallel- and orthogonal-line geometries the locations of the scatterers are estimated with less than 6% error.

When a single or small number of scatterers are present in the medium, the selection of the scattering hyperbolae is relatively easy. When many scatterers are present, as in the laboratory data, the selection of the hyperbola that belongs to the same scatterer becomes challenging, especially in case of orthogonal lines. For parallel receiver lines using the apices observed around the same receiver locations could overcome these difficulties. Another practical solution can be to perform inversion. If hyperbolas corresponding to different scatterers are selected, the observed and the calculated travel-time curves will not match and this will indicate that the hyperbolas are not representing the same scatterer. In this case another potential scattering hyperbola can be considered for location purposes. In case of a single receiver line located to one side of a scatterer, the location estimations are still possible with less accuracy.

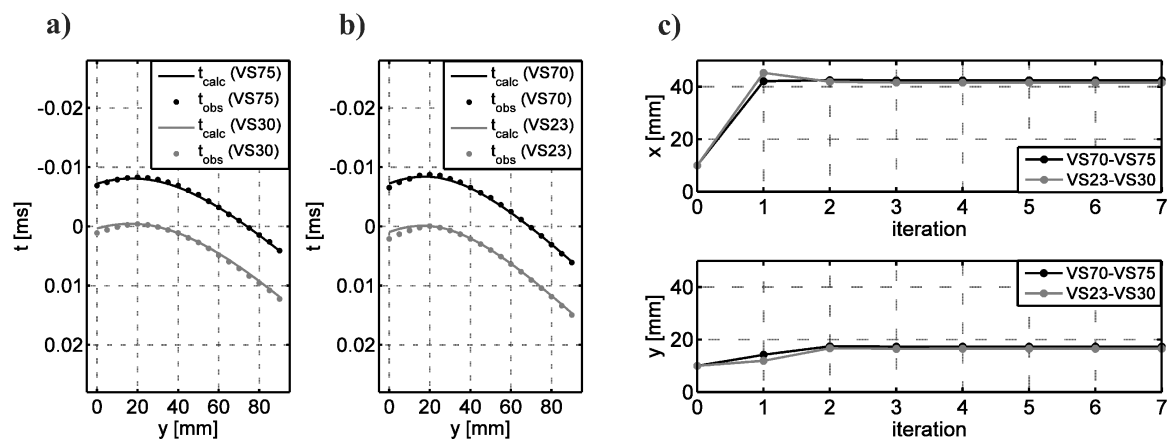


Figure 4. (a) and (b) Observed (dots) and calculated (solid line) travel times; (c) Estimated horizontal locations (x and y) of the scatterer for the virtual sources couples. The values at the zeroth iteration correspond to the initial parameters for the inversion.

Conclusions

Using a method inspired by seismic interferometry, we showed that by the correlation of scattered Rayleigh waves we can estimate the location of the scatterers. Here, we use an open boundary of receivers along two lines and one source. We show how the location of a scatterer can be estimated using data from a scaled ultrasonic experiment. As the scatterers are off the line of the receivers, two receiver lines are required to locate the scatterers. Provided that the scattered wave fields selected from the two receiver lines are representing the same scatterer and are well isolated from the total wave field, we can estimate a scatterer's location with good accuracy. An important advantage of the presented technique is that the method is independent of the wave propagation from the source to the scatterer. We foresee application of the method in wave scattering problems.

Table I. The estimated model parameters for different records (Line #) and virtual-source (VS #) locations for the configuration given in Figure 1. The actual location of the scatterer (AL), the estimated parameters (x and y) with their 95% confidence levels (1.96σ), percentage errors on the travel times (E_t) and model parameters (E_m) are also given.

Line #	VS #	AL [mm] x / y	$x \pm \sigma_x$ [mm]	$y \pm \sigma_y$ [mm]	E_t	E_m x / y
Scatterer 1						
2-4	75-70		42.50±0.98	17.32±0.41	0.15	1.2/1.0
2-4	30-23	43.0/17.5	41.57±1.57	16.49±0.80	0.34	3.3/5.8
Average			42.03±1.31	16.90±0.62		2.3/3.4
Scatterer 10						
2-3	15-85		30.60±0.33	62.70±0.40	0.08	2.9/1.3
2-3	58-20	31.5/63.5	29.71±0.53	63.42±0.73	0.30	5.7/0.1
Average			30.15±0.43	63.06±0.59		4.3/0.7

Acknowledgements

This work is supported by The Scientific and Technological Research Council of Turkey with the project TUBITAK CAYDAG110Y250 titled “Detecting Near-surface Scatterers by Inverse Scattering and Seismic Interferometry of Scattered Surface Waves”. A.K and U.H. gratefully acknowledge this financial support. The research of D.D. is supported by the Division for Earth and Life Sciences (ALW) with financial aid from the Netherlands Organization for Scientific Research (NWO) with VIDI grant 864.11.009.

References

- Grandjean, G. and Leparoux, D. [2004] The potential of seismic methods for detecting cavities and buried objects: experimentation at a test site. *Journal of Applied Geophysics*, **56**(2), 93-106.
- Harmankaya, U., Kaslilar, A., Thorbecke, J., Wapenaar, K. and Draganov, D. [2013] Locating near-surface scatterers using non-physical scattered waves resulting from seismic interferometry. *Journal of Applied Geophysics*, **91**, 66-81.
- Meles A. G. and A. Curtis [2013] Physical and non-physical energy in scattered wave source-receiver interferometry. *Journal of the Acoustical Society of America*, **133**(6), 3790-3801.
- Mikesell, T. D., van Wijk, K., Blum, T. E., Snieder, R. and Sato, H. [2012] Analyzing the coda from correlating scattered surface waves. *Journal of the Acoustical Society of America*, **131**(3), EL275-EL281.
- Mikesell, T. D., van Wijk, K., Calvert A. and Haney, M. [2009]. The virtual refraction: useful spurious energy in seismic interferometry. *Geophysics*, **74** (3) A13-A17.
- Rickers, F., Fichtner, A. and Trampert, J. [2012] Imaging mantle plumes with instantaneous phase measurements of diffracted waves. *Geophysical Journal International*, **190**, 650–664.
- Snieder, R. and Nolet, G. [1987] Linearized scattering of surface waves on a spherical Earth. *Journal of Geophysics*, **61**, 55-63.
- Xia, J., Nyquist, J. E., Xu, Y. X., Roth, M. J. S. and Miller, R. D. [2007] Feasibility of detecting near-surface feature with Rayleigh-wave diffraction. *Journal of Applied Geophysics*, **62** (3), 244-253.